MODEL COMPARISON AND VERI F1CATION FOR SC1NT1LLATION, FADE D[JRATION, AND CLOUD EFFECTS

BRADLEY E. JAEGER, I) ONAI/I) L. HOPKINS, DAE HONG KIM, AND CHARLES E. MAYER

I. Scintillations

Scintillation) model predictions were compared to **fear** years of the Fairbanks ACTS **data** at 20.2 **and 27.5** GHz. Models used in the **comparison** are Karasawa **et** al. **[1]**, ITU-R **[2],** Ortgies-N [3], Ortgies-T **[3],** DPSP (Direct Physical **Statistical Prediction)** [3], MPSP **(Modeled** Physical **Statistical** Prediction) **[3],** and Tervonen et **al. [4].** Dependencies of these seven models are shown in **'1'able 1.** The **monthly** average for **scintillation** standard deviation, along with **all** the **model predictions** using **the local meteorological** parameter input, **is plotted** in Figs. 1 and **2** for **20.2** and **27.5** GHz respectively.

TABLE 1. SCINTILLATION MODEI, COMPARISON

Scintillation Model	Year	freq dep.	sin() dep.	Par	H (m)	Data source	Regression	Model Restrictions	Fade/ Enhan.
Karasawa, Yamada, Allnutt	1988	0.45	-1.3	N_{wet}	2000	Yamaguchi, Japan (1 1.45 (ill/. 4,().5,9")	m vs. N_{wet}	7-14 (ill/ 4 ~ 0 ~ 30""	Regres. ill vs. variance
ITU - R	1990	0.583 (7/12)	-1.2	N_{wet}	1 000			6 - 20 (ill/ 4 o 30°	Regres.
Ortgies-N	1993	0,005	-1.2	N_{wet}	1000	Darmstadt, Ger. (Oly)	$\ln(\sigma_x^2)$ vs. N_{wet}	6.5 o 30""	∫ Gauss. (sym.)
Ortgies-T	1993	0.605	-1.2	'1	1000	-Darmstadt, Ger.(Oly)	Ill(σT^2) vs. '1'	6.5 0 30°	∫ Gauss. (sym.)
DPSP- Direct Physical Statistical Prediction	1997	0.583	-1,2	'I	205X -1 94.5 '1'	Louvain-la-Neuve, Bel. (12.5, 29.7) and Milan, Italy (19.8)	Ver. Refrac. gradient (radiosonde) to give $\ln(\sigma_x^2)$ vs. 'I	'1 ~ -5 C	∫ Gauss. (sym.)
MPSI - Modeled Physical Statistical Prediction	1997	0.583	-.917	'I	2058 -1 94,5 '1'	Louvain-la-Neuve, Bel. (12.5, 29.7) and Milan, Italy (19.8)	Ver Refrac. gradient (radiosonde) to give $\ln(\sigma_x^2)$ vs. '1	'I ~ -5 C	∫ Gauss. (sym.)
1ervonen, van de Kamp, Salonen	1998	0.45	-1.3	N_{wet} P(C	2000	Kirkkonummi, Finland (19.X. 29.7)	σ_x vs. N_{wet} & P(Cu)		

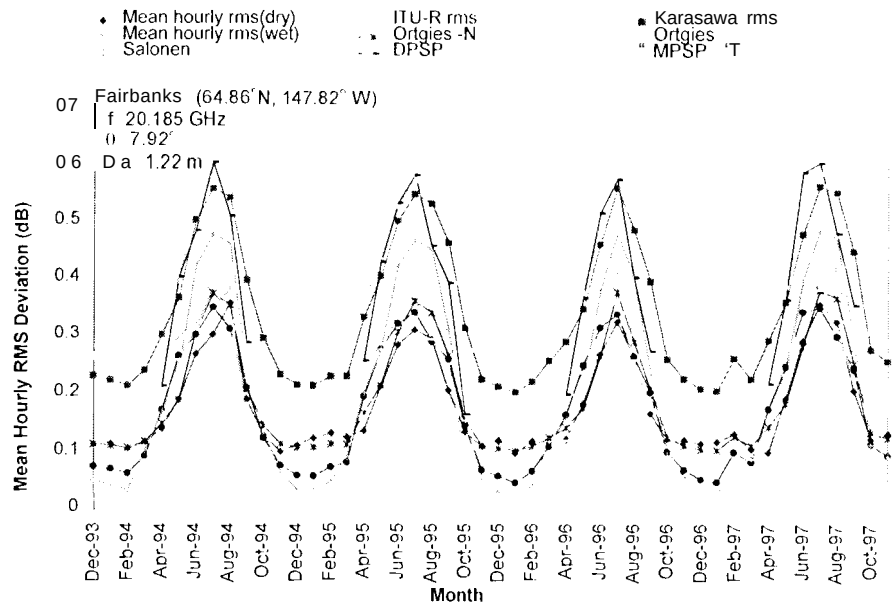

Fig. 1. 4 Year Comparison of Monthly Average 20 GHz RMS Deviation With Model Predictions

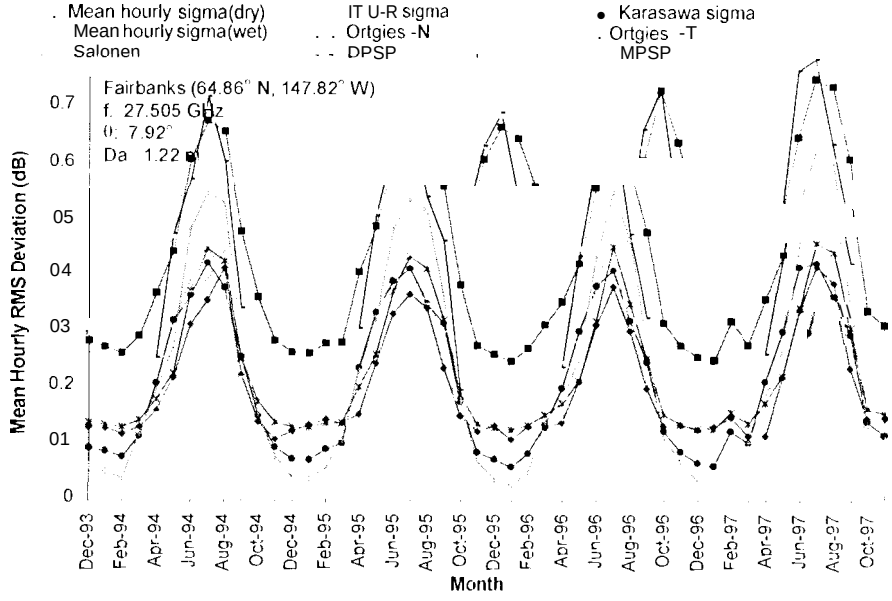

Fig. 2. 4 Year Comparison of Monthly Average 27 GHz RMS Deviation With Model Predictions

II. Matricciani Fade Model

'I'able 2 **indicates** the **place** of the Matricciani **lade model** among other models of fade durations. The data **used** in the development of each model **arc** listed along with **the basic** modeling technique. The Matricciani model **is** not an engineering model since **it** requires the user to have a rain rate time series but **it** may provide better prediction accuracy than other models. **It is mostly a** mathematical construction with only storm **translation speed,** v, obtained from radar measurements in northern **Italy.** Compared to **other fade** duration **II** rodels it also has the advantage of being able to predict fade **times. At** present, the only other model to do **this is tile** Paraboni and Riva model.

TABLE 2. FADE DURATION MODEL COMPARISON

Model	Data Frequenc	[kits Location	Model 'Type	Engineerii Model	Accoui for sho fades	Prec Fad Tim
Matricciani [6], [71		Po River Valley	Simulation with Synthetic Storm Technique	No	No	Yes
Paraboni & Riva [1 O]	11.6 GHz ITU Database	Fucino, Gera Lario, Spino d'Adda	Log-normal Long Durations Power-Law Short Durations	Yes	Yes	Yes
ACTS Rain Prediction Model [11], [12]	NA	NA	Log-normal Attenuation Spatial Correlation of Rain Cells Probability of Rain on the Path 2-dimensional Markov Process.	Yes	Yes (Rain)	No
Maseng & Bakken [13]	NA	NA	Log-normal Attenuation. 1-dimensional Markov Process	No	Yes (Rain)	No

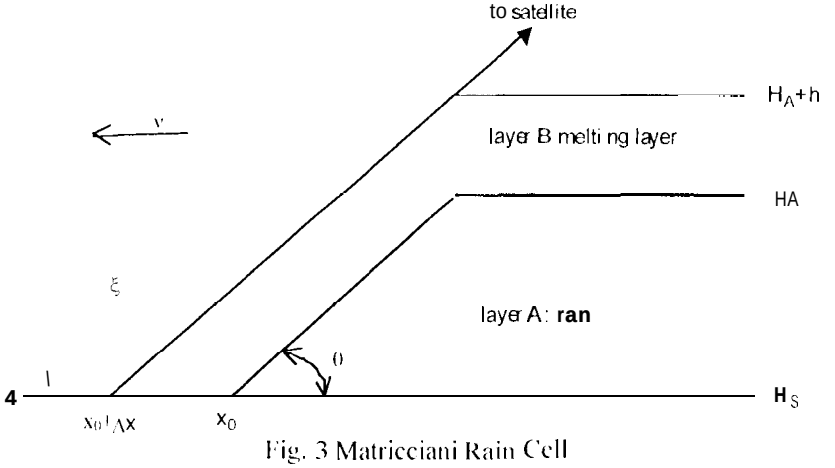

Fig. 3 Matricciani Rain Cell

Fig. 3 shows the precipitation pattern used in the Matricciani fade model. The cell is rectangular with a layer of rain at 20° C and a melting layer at 0° (. The variation in attenuation with time is simulated by the convolution of a function of rectangular shape with specific attenuation from a rain rate time series. In the Matricciani model, this convolution is done using a product in the frequency domain.

$$\breve{S}_A(f) = \breve{S}_{Y,A}(f) \cdot L_A \cdot \sin c\left(f \cdot L_A / v(\theta)\right) \cdot \exp\left(-j \cdot 2 \cdot \pi \cdot f \cdot \Delta x_0 / v(\theta)\right)$$
$$+ r^{\alpha_R} \cdot \breve{S}_{Y,B}(f) \cdot \Delta L \cdot \sin c\left(f \cdot \Delta L / v(\theta)\right) \quad (1)$$

The sinc functions result from the rectangular cell and the exponential is a shift due to the difference in path lengths, Δx. 'The is an extra term r^{α_R} to account for the extra attenuation due to the melting layer. The simulated attenuation time series is then the inverse Fourier transform of (1). Fade durations greater than 60 seconds were then calculated from this attenuation time series. Statistics were recorded for the number of fades and the fade time. Since the Matricciani model attempts to account for fades from rain only, the statistics from the model were compared to statistics from measured ACA. Errors were measured for percentage of fade time and percentage Of fades. The error at a given percentage and attenuation threshold was taken as

$$\varepsilon \equiv \ln\left(\frac{FD_{ACA}}{FD_{Matricciani}}\right) \quad (2)$$

Table 3 gives a summary of these errors for four years of Fairbanks data

TABLE 3. MATRICCIANI MODEL ERRORS (DECEMBER, 1993 - NOVEMBER, 1997)

	Number of Fades								Fade Time							
	1 dB	ACA 3 dB	ACA 5 dB	ACA 7 dB	ACA	1 dB	ACA 3 dB	ACA 5 dB	ACA 7 dB	ACA						
20 GHz avg	0.022558	-0.01084	0019154	0.033059		0.014517	0.022338	0.028899	0.027749							
20 GHz rms	0.071022	0055106	0.087449	0088875		0.062319	007034	0082712	0.072792							
27 GHz avg	0.037327	0.047002	0031158	0.0655		0.014491	0.022303	0.022052	0.049574							
27 GHz rms	0.143646	0.09891	0.075965	0.14493		0.12134	0.072475	0.077938	0.126067							

The positive signs in front of errors in table 3 indicate that in all but one case the Matricciannı model underpredicts troth the number Of fades and the fade time. Fig. 4 and 5 show graphically how well the Matricciannı model predicts number oi'fades and fade time at 27.505 GIIz for a representative year in Fairbanks, December 1996-November 1997.

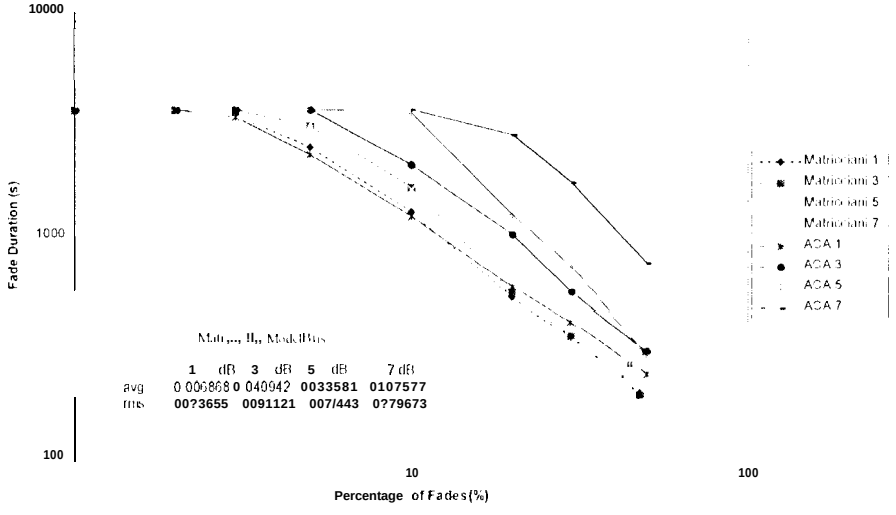

Fig. 4 - Number of 27 GHz ACA Fades Compared to the Matricciani Model.

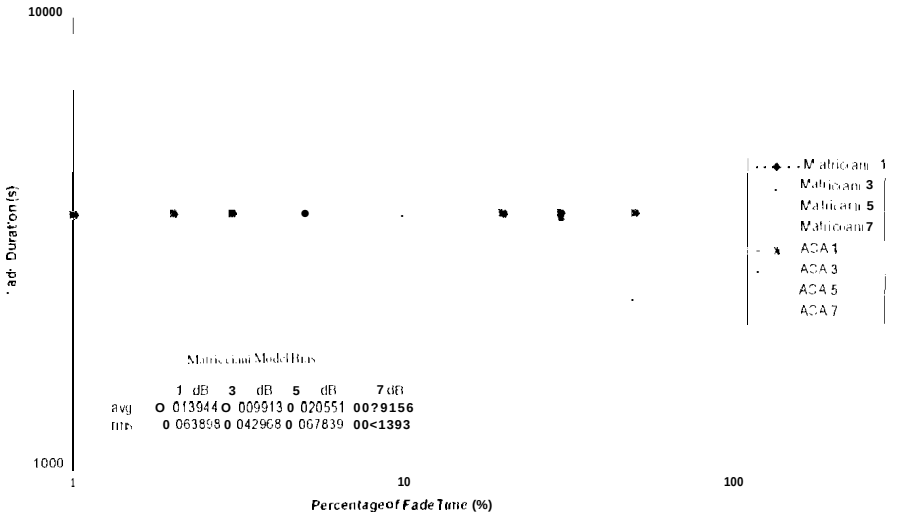

Fig. 5 . 27 GHz ACA Fade Time Compared to the Matriccianni Model.

Fig. **6** shows attenuation cumulative distribution function for the Matriccianni model compared to an ACA cd f at 27.505 GHz for **a** representative month **at** Fairbanks. The two dashed **carves arc** model curves. There **is** one for **Optical gauge** rain rate, ORR, and one for **capacitive** gauge rain rate, CRR. The **A('A** curves **fall** above **tile** model curve for low attenuations. **It** may be that if the Matricciani model **had a** development accounting for antenna **wetting** this discrepancy would be resolved.

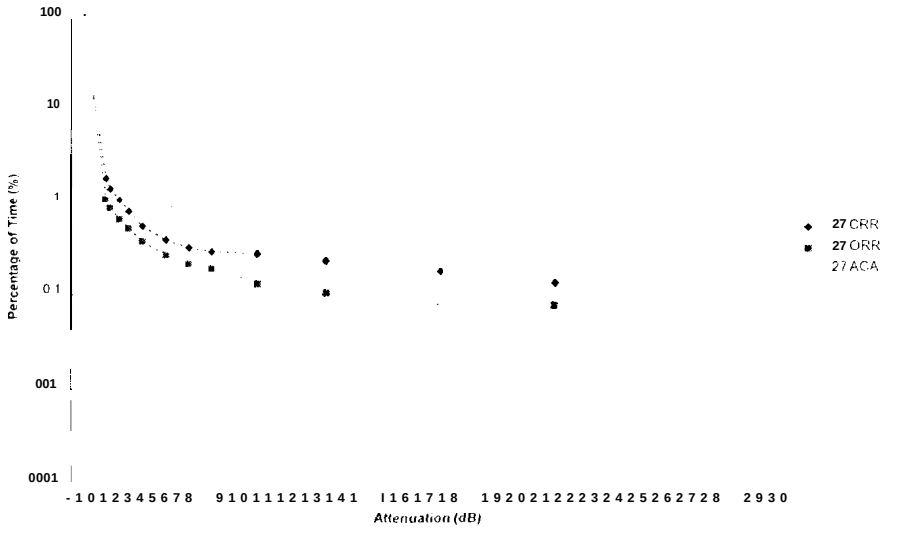

Fig. 6 - (June, **1997)** 27.505 GHz ACA Compared to **the** Matricciani Model.

III. ACTS Data Correlated to Gaseous, Rain, and Cloud Attenuation Models

This section explores correlation of received ACTS beacon values to atmospheric attenuation by adapting National Climatological Data Center (NCDC) data used in clear sky (gaseous), rain, and cloud attenuation models. Attenuation due to clear sky and rain utilize ITU-R semi-empirical attenuation models, however cloud attenuation is more difficult to model clue to highly variable cloud structures. Prior to July 1996, NCDC cloud cover data is recorded in tenths of total cover, with 10/1 0 = total cover. After June 96 NCDC recorded cloud data format changed, listing only five cloud cover increments: O (SKC or CLR), 1/8- 1/4 (FEW), 3/8-1/2 (SCT), 5/8-7/8 (BKN), and 8/8 (OVC), and up to four distinct cloud ceilings. Cloud attenuation models arc investigated, but require knowledge 01'the density of water (g/m^3) along the propagation path, which is generally not known. A SkyCam (modified digital camera) is used to help correlate viewed cloud conditions to NCDC published values. This section will show how recorded ACTS propagation data compares to the sum of attenuation from the three propagation models.

A. ACTS Data Collection Procedure

The first step in the analysis is to collect ACTS data in a from, which will allow comparisons over along period. '1'0 accomplish this, a special program (1 hilcxt3.exe) was developed by Dave Westenhaver of Westenhaver Wizard Works to take preprocessed ACTS data and extract only the first minute of data (60 samples) from each hour selected. After this data is extracted, the next step is to limit the range Of data to values greater than a threshold Of- I 9 dB. This threshold is chosen since any values lower than this are considered below the noise floor of the equipment. After these erroneous values are eliminated, the remaining values for the minute are manipulated, where the average, maximum, and minimum values are saved for use in attenuation and scintillation studies. Finally the values (one per hour from hh:00:00 to hh:00:59) are collected and placed into a set of yearly ACTS averaged data for usc in EXCEL. Averaging, saving maximum/minimum values, and compiling the data is done via an EXCEL macro specially developed for this purpose. Fig. 7 shows pictorially the data collection process and a sample of the collected data.

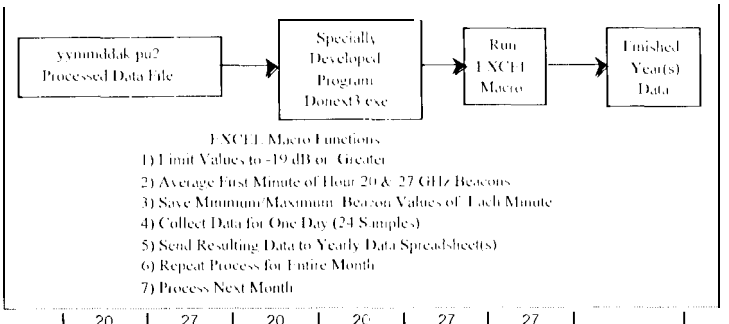

	20 Beacon Average	27 Beacon Average	20 Beacon Min	20 Beacon Max	27 Beacon Min	27 Beacon Max	20 Scintillation	27 Scintillation
1/1/97 0:00	-0.5	-0.7	-0.23	-0.51	-0.42	-0.74	0.28	0.32
1/1/97 1:00	-0.5	-0.66	-0.41	-0.77	-0.63	-0.95	0.36	0.32
1/1/97 2:00	-0.67	-0.98	-0.34	-0.69	-0.55	-0.98	0.35	0.43
1/1/97 3:00	-0.35	-0.49	-0.29	-0.61	-0.47	-0.87	0.32	0.4
1/1/97 4:00	-0.25	-0.42	-0.08	-0.48	-0.28	-0.69	0.4	0.41
1/1/97 5:00	-0.38	-0.53	-0.25	-0.57	-0.49	-0.74	0.32	0.25
1/1/97 6:00	-0.5	-0.68	-0.35	-0.69	-0.58	-0.82	0.34	0.24
1/1/97 7:00	-0.53	-0.76	-0.32	-0.59	-0.5	-0.81	0.27	0.31
1/1/97 8:00	-0.56	-0.73	-0.23	-0.65	-0.56	-0.93	0.42	0.37
1/1/97 9:00	-0.46	-0.62	-0.44	-0.82	-0.53	-0.99	0.38	0.46
1/1/97 10:00	-0.31	-0.45	-0.23	-0.67	-0.31	-0.81	0.44	0.5
1/1/97 11:00	-0.51	-0.57	-0.12	-0.56	-0.26	-0.71	0.44	0.45
1/1/97 12:00	-0.12	-0.53	-0.12	-0.71	-0.47	-1.03	0.59	0.56

Fig 7 - Conversion of Processed ACTS Beacon Data to EXCEL Data

B. Compiling NCDC Weather Data Used In The Analysis

Once the data is collected, the next step is to compile a set Of weather data for the Fairbanks area. Required weather data used in the attenuation models includes: temperature (°C), relative humidity (o/o), rain rate (mm/hr), cloud cover (10^{ths}), and cloud ceiling (m). NCDC weather data is published monthly (with about a one-month delay) and is available to users from any local National Weather Service office in print form and is also available on a fee basis via the Internet. One exception to the fcc based data requires an educational (.edu) address on the requester's internet server. Of course other sources of local weather data exist. For this analysis much of the data is collected from a CD published by NOAA and available at the UAF's Rasmussen library. A variety of weather data is available in hourly readings/summaries (including many Of the required types) for years up to 1995. Data is recorded using local standard time and correlation to ACTS data requites an appropriate time shift. The only weather parameter required for the attenuation models not included is rain rate, however the total accumulation is included for the preceding hour in the data. In this analysis rain rate is estimated as (total accumulation for the hour)/(one-hour), giving an estimated rain rate for each sample period.

C. Modeling of Gaseous Attenuation

The first clement of the analysis is to model the gaseous attenuation for the ACTS to Fairbanks slant path. The gaseous (clear-sky) attenuation model is by the CCIR (1990) in Report 719 [14], which is a semi-cmpirica! model used to estimate the amount Of gaseous attenuation. This model takes into account atmospheric gases attenuating effects due to oxygen and water vapor (not including water vapor in cloud structures). This commonly referenced attenuation model utilizes signal and weather data including:

f Frequency (GHz)
T Temperature (°C)
θ Elevation angle (rad)
ρ Water Vapor Density (g/m^3)
RH Relative Humidity (%)
Rain yes/no (relates to scale height of ρ)

Calculations used in the gaseous attenuation analysis are included in Appendix B. once the attenuation values are calculated, they are placed into a spreadsheet and correlated to the averaged ACTS beacon values. Fig. 8 shows the results of the comparison. Note the seasonal trends show nicely on the plots, but deep fades are not tracked since they are due to rain attenuation, studied next. Also note the correlation coefficients shown in the plots where the 20 GHz (89.1%) is better correlated than the 27 GHz (76.7%). This difference is mainly due to the higher variability of the 27 GHz signal.

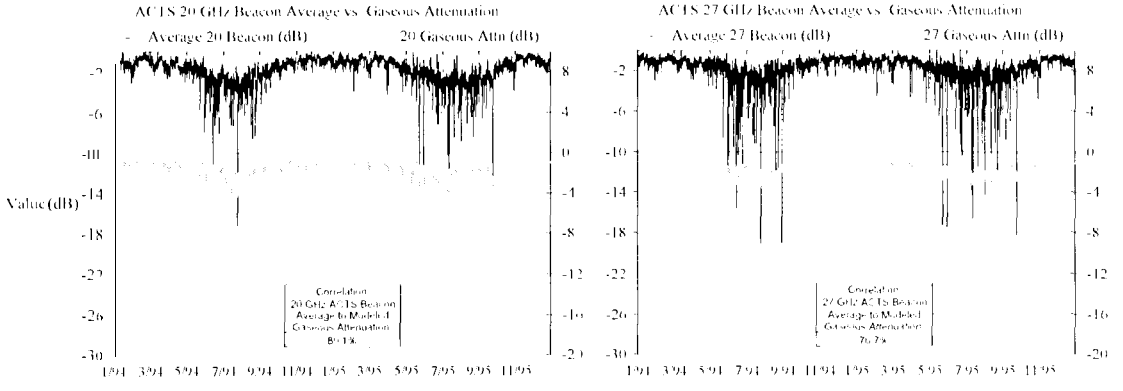

Fig 8 - Gaseous Attenuation vs. Averaged ACTS Beacon Values

D. Modeling of Rain Attenuation

Rain is the most severe attenuating factors in radiowave propagation, especially at higher frequencies. Even though this is the case, accurate measurement of rain rate (usually measured in mm/hr) during a rain event are not easily obtained. Errors exist from many sources including spatial diversity where the rain is falling in the propagation path, but not at the measurement site. Fig. 9 [I 5] shows sources of error for horizontal(L_H) and vertical(L_V). In addition most conductive rain cells have widely varying amounts of rain rates throughout the cell and the rain gauge is usually at one position. In this instance there are errors induced, since NCDC data is used as the source of rain talc data and the Fairbanks weather station is approximately 3 km from the ACTS terminal.

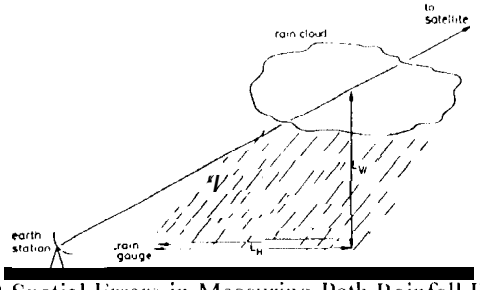

Fig. 9 Spatial Errors in Measuring Path Rainfall Rate

Now given a rain rate (approximated as total rain for the hour per hour) the only missing variable in the equation is the effective path length. For this approximation another piece of information is necessary, rain elevation within the cloud layer. Initially it was hoped that NCDC cloud ceiling represented the bottom of the rain, however published values did not seem to relate to the heights of rain-bearing clouds. Also values for cloud ceiling are not consistently available, so ITU recommendation RPN.6 I 8-4, I 996 gives a method to estimate the effective slant path length of the rain layer below the freezing height. Calculations required to estimate rain attenuation arc shown in Appendix C, where only knowledge of station latitude is required to estimate the effective rain path [I 6].

One approximation made is there will be no rain, although there may be snow, for ground temperatures less than I 'C. Liquid water in the form Of rain is a strong attenuator Of radio waves at ACTS frequencies, whereas snow mainly attributes to depolarization, which is not easily extracted from the ACTS data. NCDC data shows equivalent precipitation and does not differentiate this rain from snow. Luckily the transition Of rain to snow occurs over a short period 6f the year in Fairbanks and should not skew the approximation significantly. Also to help account for the estimated rain rate experienced during the sampled period a value of I.3 times the hourly rain accumulation from the NCDC data adjusts the hourly rate to a empirically defined rate (mm/hr) for the sample period. This I.3 factor is determined from looking at the differences between the modeled gaseous + rain attenuation values, where the correlation Of the two data sets is minimized for attenuation greater than 3 dB. Without more accurate radiosonde m real time rain rate data available, this approximation will certainly include errors, but the goal is to determine if NCDC data is usable to estimate rain attenuation with any degree of accuracy. Fig. I O shows the results Of the comparison, including modeled gaseous and rain attenuation.

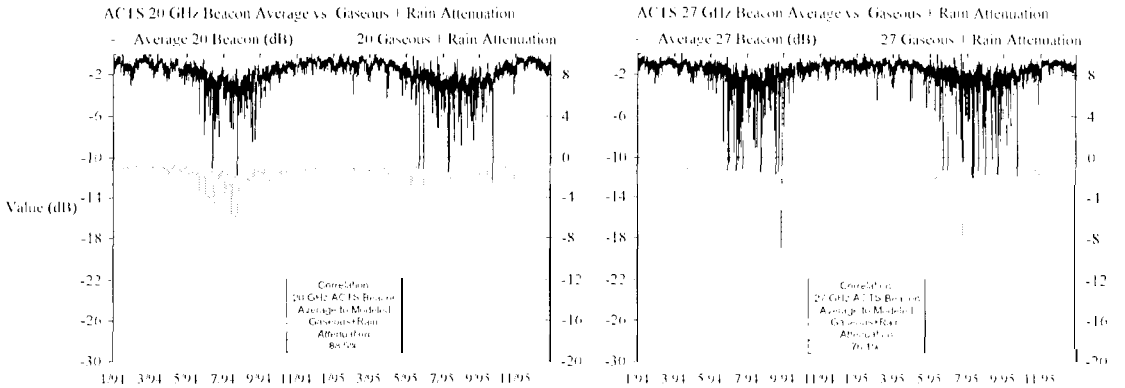

Fig 10 - Gaseous + Rain Attenuation vs. Averaged ACTS Beacon Values

It is **interesting** to note in Fig. **I O** the **deep fades,** although not **exactly** correlated to the ACTS **data,** provide **a** better **estimate** of the actual performance of the **satellite** link **based** on the two models. One surprising result **is** the correlation of the two data sets did not improve with **the** added attenuating factor; in **fact** the correlation **is slightly** worse, 20 GHz from 89.**I** 0/0 to **88.90/0** and **27** GHz from **76.7°/0** to **76. 10/O.** This **is** probably due to an assumed **"mismatch"** of the **estimated** rain **data** and **the** ACTS beacon data. An analysis of the differences between **the** modeled attenuation and the actual ACTS data **is** performed using an absolute difference between the two **values** and **calculating** the differences in percent **Of** `total. This comparison **is** shown in Fig. **11.** Note a **difference** of only 2 dB **excludes all** but **0.78% at** 20 GHz and **all** but 1.81% at **27** GHz.

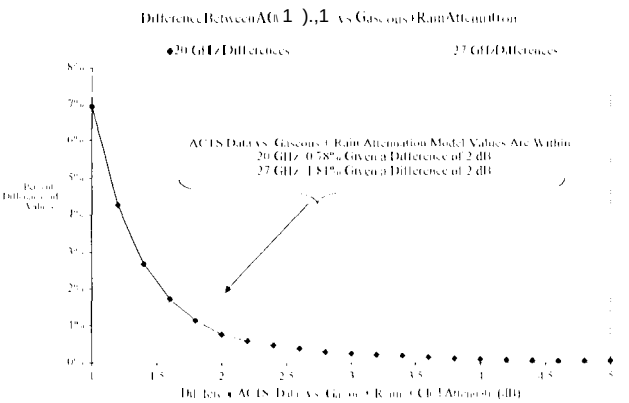

Fig 11 - Compare Gaseous + Rain Attenuation vs. Averaged ACTS Beacon Values

The **overall** trends in Fig. **10** show a **slight** discrepancy between the ACTS beacon values and the gaseous + rain attenuation models (like a **de Off-set)** for **the** summer months, thus in **the** next section **a** cloud attenuation model **is** defined to **help** counteract **this.**

E. Modeling of Cloud Attenuation

The attenuating effects of clouds on a satellite link may not have as dramatic effect as the gaseous or rain attenuation, but clouds may be present for a significant amount of time in the propagation path. Rain on the other hand is usually limited to short-term duration events. Clouds contain a combination Of suspended water droplets and if conditions allow icc crystals. The suspended water droplets change the dielectric properties of the propagation path and effect via absorption/scattering the propagating radiowave. '1 0 begin with an analysis of various types 01' clouds generally observed and their inherent properties is appropriate.

Haroules and Brown measured cloud attenuation in I 969 [1 7] at frequencies Of 8, I 5, 19, and 35 GHz also at frequencies of 15 and 35 GHz by Alshuler. Using these studies and others, water density Of many cloud types has been estimated. Slobin [I 7] lists typical parameters of clouds in mid-latitude conditions. This approximation is not truly suited for Alaska conditions, however during the summer in Fairbanks many of the cloud structures present are similar to those described. The next element in any model are the equations necessary to predict cloud attenuation. E. Salonen and S. Uppala [I 8] formed a model to predict the specific attenuation Of clouds for frequencies above 20 GHz. Their model is based on Liebe's M1'M model [19]. '1 he evaluation of this model uses the parameters shown in Appendix D.

Next Fig. 12 shows Slobin's results and lists 15 different cloud types at mid-latitudes, their specific water density (g/m^3), and typical heights above the ground (m) for top and bottom Of each type Of the 15 types Of cloud structures. These I 5 cloud types are grouped and adjusted such that the parameters for each cloud type (specific water density (g/m^3) and effective depth) when evaluated using tile equations in Appendix D, represent attenuation values observed by correlating ACTS data and Sky Cam views, discussed in the next section. Note in Fig. 12, effective path is only an estimate using estimated top and bottom as a guide

Slobin's Cloud Types

Cloud Type	Density (g/m3)	Height Above Ground (m) Bottom	Top
Heavy Fog 1	0.37	0	150
Heavy Fog 2	0.19	0	150
Moderate Fog 1	0.06	0	75
Moderate Fog 2	0.02	0	75
Cumulus	1.00	660	2700
Altostratus	0.41	2400	2900
Stratocumulus	0.55	660	1320
Nimbostratus	0.61	160	1000
Stratus	0.42	160	660
Stratus	0.29	330	1000
Stratus-stratocumulus	0.15	660	2000
Stratocumulus	0.30	160	660
Nimbostratus	0.65	660	2700
Cumulus-cumulus congestus	0.57	660	3400

New Cloud Models

Cloud Type	% Coverage	Density (g/m3)	Height Above Ground (m) Bottom	Top	Effective Path (m)
Stratus	0.8 1.0	0.1.	2 1 5	8 5 0	1 1 0
Stratocumulu	0.[illegible]	0.1.	8 3 8	1 1 2 5	mm
Nimbostratus	0.8 1.0	0.32	1 1 0	1 8 6 0	5 0 0
Cumulu	0.2 - 0.5?	0.38	6 6 0	3 0 5	7 0
Altostratus	[illegible]	0.21	2 4 0 0	2 9 0	5 1 0

Fig 12- Conversion of Slobin's 15 Cloud Types to New Model Cloud Types

Next the NCDC data is adapted to convert specific cloud coverage and ceiling data to these newly defined cloud types and then the calculations for cloud attenuation are performed. Fig. I 3 shows a flowchart Of how the clouds arc classified and the parameters used in the model.

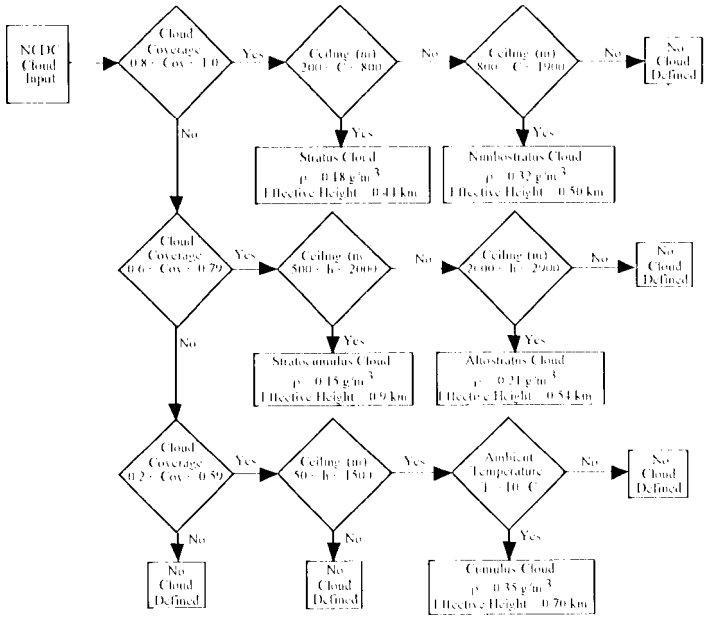

Fig 13 Flowchart of NCDC Data to New Model Cloud Types

The next step is to calculate the attenuation clue to clouds, then add this attenuation to gaseous and rain attenuation values, calculated earlier. Fig. 14 shows the results of this comparison. Note in this figure the dc offset noted earlier is not observed.

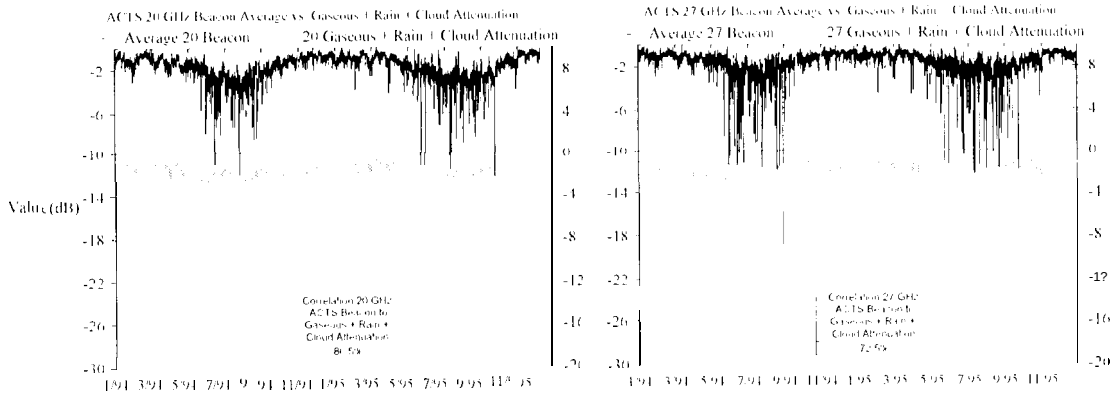

Fig 14 Gaseous + Rain + Cloud Attenuation vs. Averaged ACTS Beacon Values

Again an **analysis** of the differences between the modeled attenuation and actual ACTS data **is** performed using an absolute **difference** between the two values and **calculating** the differences in percent of total. This comparison **is** shown in Fig. **15.** Note a difference of only 2 dB excludes **all** but 0.62% **at 20** GHz and all but **1 .320/0** at 27 GHz, an improvement over the model with only gaseous and rain attenuation values. The final comparison **is** when smaller time frames (one **day)** of three-part attenuation **is** correlated with the ACTS data. This comparison **is** shown next.

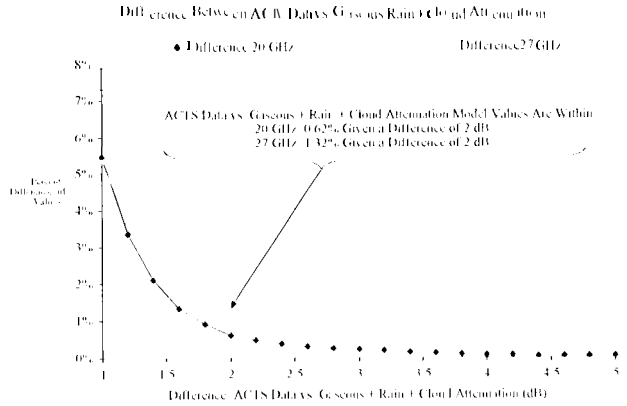

Fig 15 - Compare Gaseous + Rain Attenuation vs. Averaged ACTS Beacon Values

F. Comparison of One-Day Cloud Attenuation for Various Cloud Types

To ensure an accurate evaluation of cloud attenuation, a SkyCam is used to capture sky views and these views are used to coordinate cloud structures with observed ACTS attenuation. A sample of the SkyCam views and a schematic of the SkyCam apparatus are shown in Fig.16.

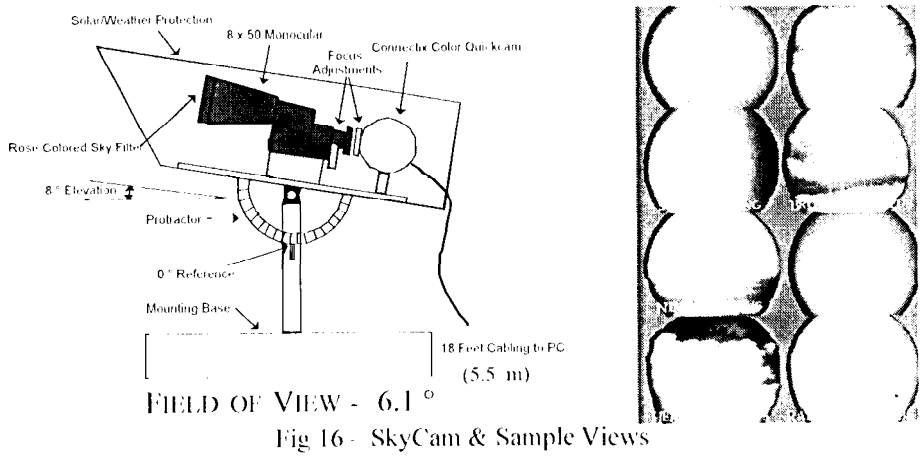

Fig 16 - SkyCam & Sample Views

The first type of cloud structure examined is that of cumulus clouds at/above cloud ceiling of 1500 meters. Fig. 17 shows the correlation of the ACTS beacons with the modeled attenuation. Also shown is the differences of the models with and without cloud attenuation and whether the models under or over predict the actual averaged ACTS attenuation. The curves on the right portion of the plot are when rain occurred in the signal path; otherwise where the cloud is noted the modeled attenuation tracks well with the actual data.

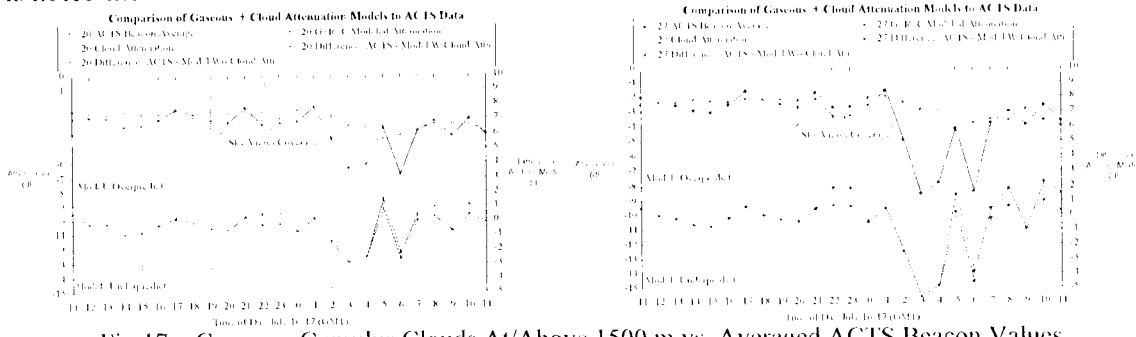

Fig 17 - Compare Cumulus Clouds At/Above 1500 m vs. Averaged ACTS Beacon Values

Another type Of cloud is that of a cumulus at a lower elevation, however this time about the cloud is at a ceiling of 500 meters and there is no rain present in the path. The comparison for this type of NCDC defined cloud type is shown in Fig. 18. Note in this case addition of cloud attenuation alters the difference and provides a better fit to the ACTS data.

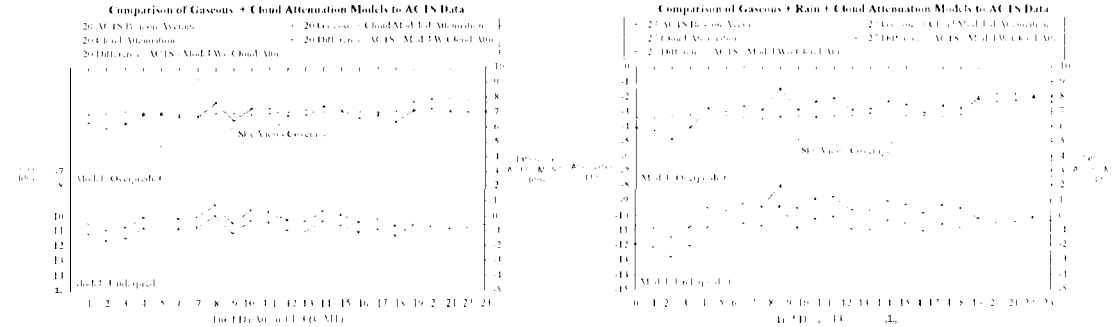

Fig 18 Compare Cumulus Clouds At 5(K) m W/o Rain vs. Averaged ACTS Beacon Values

Another type of cloud examined is that of a stratocumulus. Fig. 19 shows the comparisons for this type of cloud structure. Again the addition of the cloud attenuation improves the fit to the recorded ACTS data.

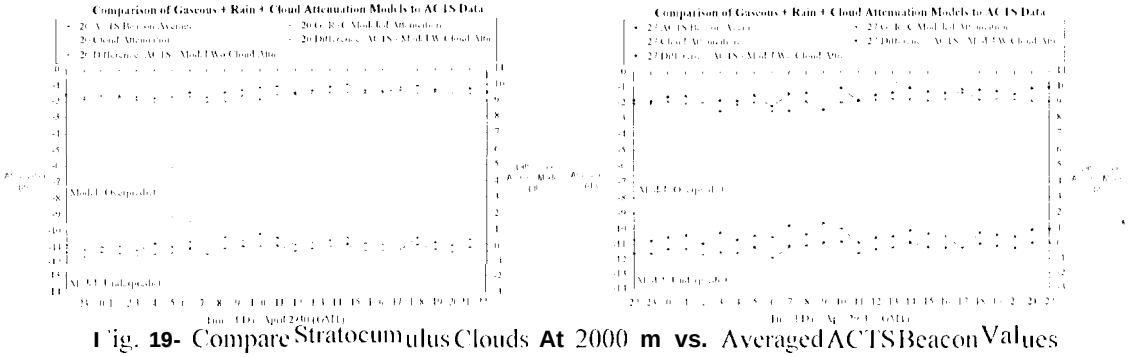

I Fig. 19- Compare Stratocumulus Clouds At 2000 m vs. Averaged ACTS Beacon Values

The final type of cloud examined is that of an altostratus. This comparison is shown in Fig. 20. In this case the cloud attenuation is not of significant effect and does not significantly improve the fit.

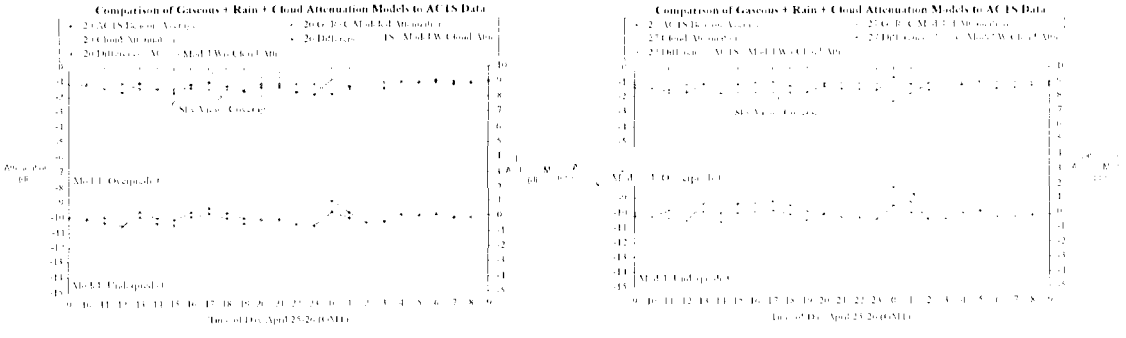

Fig. 20 Compare Altostratus Clouds 2000 < h < 2900 m vs. Averaged ACTS Beacon Values

(i. Statistical Analysis of the Model\

Up until now the values of attenuation have been evaluated relative to the ACTS averaged beacons, however many systems designers like to see statistics on tile data. To compile a statistical analysis the Averaged ACTS beacon value.s are divided into 'bins' where values greater than a set attenuation value are collected and then a percentage is taken over the data set total, this is commonly known as a CDF. Fig. 2 1 shows the set of CDF data collected for the three types of modeled attenuation and the of the averaged ACTS data. As is shown in the figure, the 27 (if Iz models indeed do a very good job of predicting the attenuation of the ACTS-to-Fairbanks although the 20 GIIz comparison is not as good, still represents a fair estimate Of the link propagation statistics.

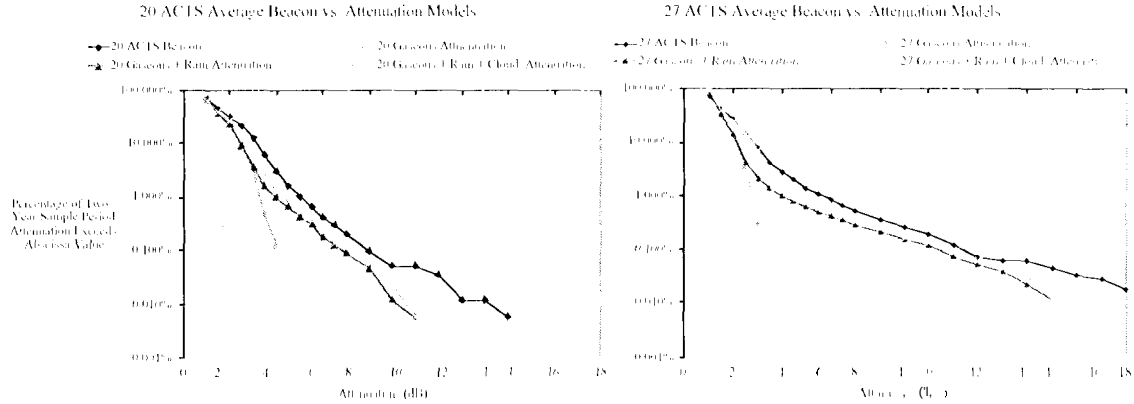

Fig. 21 -- CDF of ACTS Averaged Beacons vs. Modeled Attenuation

IV. Conclusions

The Ortgies-N scintillation prediction model best matches the ACTS data at Fairbanks, out of the seven models that wc examined.

The Matricciani fade model was shown to underpredict both the number of fades and fade time for clear air attenuation. Subjectively, the magnitudes of the prediction errors are smaller for this model than for other fade prediction models.

In this study it is shown how NCDC weather data may be used with accepted CCIR gaseous and rain attenuation models and do a good job of estimating the actual ACTS performance for the ACTS to Fairbanks link. However with the addition of an empirically defined cloud attenuation model, the data fit is even better. Individual cloud types are examined and attenuation during specific cloud occurrences is determined. An interesting conclusion is that while the additional cloud attenuation by itself is not significant (when compared to gaseous and rain attenuation), it provides enough adjustment to improve the overall CDF. The end result is that given easily available NCDC weather data (with slight alterations), and CCIR gaseous and rain attenuation models along with an empirically defined cloud attenuation model, a reasonable prediction of the performance of satellite to ground propagation characteristics at ACTS frequencies can be made.

APPENDIX A - Calculation of Power Law Parameters for Matricciani Fade Duration Model at Fairbanks

ϕ (14, 86

h 0.4

$H_s(\phi) := 5.0 - 0.075 \cdot (\phi - 23.0)$

$H(\phi) := H_s(\phi) - h$

$H = 0.13716$

$\theta := \frac{7.92 \cdot 2\pi}{360}$

$L := \frac{H(\phi)}{\sin(\theta)}$ H

$L_s := \frac{H_s(\phi)}{\sin(\theta)}$ H

π 3.134

$\frac{h}{\tan(\theta)}$

$\alpha := \frac{64.86 \cdot 2 \cdot \pi}{360}$

$\beta := \frac{(260 - (360 - 147.82)) \cdot 2 \cdot \pi}{30(\text{I}}$

$\tau := a\tan\left(\frac{\tan(\alpha)}{\tan(\beta)}\right)$

Using Maggiori[9] power law parameters for 20 °C at 20, 25, and 30 GHz the interpolations for 20.185 and 27.505 GHz are:

$$kh20 := 10^{\left(\log\left(\frac{.124}{.0751}\right)\cdot\frac{\log\left(\frac{20.185}{20}\right)}{\log\left(\frac{25}{20}\right)}+\log(0.0751)\right)}$$

$$kv20 := 10^{\left(\log\left(\frac{.113}{.0691}\right)\cdot\frac{\log\left(\frac{20.185}{20}\right)}{\log\left(\frac{25}{20}\right)}+\log(0.0691)\right)}$$

$$\alpha h20 := (1.061 - 1.099)\cdot\frac{\log\left(\frac{20.185}{20}\right)}{\log\left(\frac{25}{20}\right)} + 1.099$$

$$\alpha v20 := (1.03 - 1.065)\cdot\frac{\log\left(\frac{20.185}{20}\right)}{\log\left(\frac{25}{20}\right)} + 1.065$$

$k20 \frac{(kh20\ kv20)\ \text{I}\ (kh20\ kv20)\cos(\theta)^2\cos(\tau\ \ 2\ )}{2}$

$k20 :=$ **(),() 7122(,3(,3**

$$\alpha 20 := \frac{kh20\cdot\alpha h20 + kv20\cdot\alpha v20 + (kh20\cdot\alpha h20 - kv20\cdot\alpha v20)\cdot\cos(\theta)^2\cdot\cos(2\cdot\tau)}{2\cdot k20}$$

$\alpha 20 :=$ **1.()(177()14815**

$$kh27 = 10^{\left(\log\left(\frac{.187}{.124}\right)\frac{\log\left(\frac{27.505}{25}\right)}{\log\left(\frac{30}{25}\right)}\log(0.124)\right)}$$

$$kv27 = 10^{\left(\log\left(\frac{.167}{.113}\right)\frac{\log\left(\frac{27.5(15}{25}\right)}{\log\left(\frac{30}{25}\right)}\log(0.1\ 13)\right)}$$

$$\alpha h27 = (1.021 - 1.061)\cdot - \frac{\log\left(\frac{27.505}{25}\right)}{\log\left(\frac{30}{25}\right)} + 1.061$$

$$\alpha v27 = (1.00 - 1.03)\frac{\log\left(\frac{27.505}{25}\right)}{\log\left(\frac{30}{25}\right)} + .03$$

$$k27 = \frac{(kh27 + kv27) + (kh27 - kv27)\cdot\cos(\theta)^2\cdot\cos(\tau\cdot 2)}{2}$$

$k27 = 0.1403958942$

$$\alpha 27 = \frac{kh27\cdot\alpha h27 + kv27\cdot\alpha v27 + (kh27\cdot\alpha h27 - kv27\cdot\alpha v27)\cdot\cos(\theta)^2\cdot\cos(2\cdot\tau)}{2\cdot k27}$$

$\alpha 27 = 1.0175416272$

Using Maggiori [9] power law parameters for 0 °C at 20, 25, and 30 GHz the interpolations for 20.185 and 27.505 GHz are:

$$kh20 = 10^{\left(\log\left(\frac{.1159}{.06772}\right)\frac{\log\left(\frac{20.185}{20}\right)}{\log\left(\frac{25}{20}\right)}+\log(0.06772)\right)}$$

$$kv20 = 10^{\left(\log\left(\frac{.1028}{.06097}\right)\frac{\log\left(\frac{20.185}{20}\right)}{\log\left(\frac{25}{20}\right)}+\log(0.06097)\right)}$$

$$\alpha h20 = (1.081 - 1.119)\cdot - \frac{\log\left(\frac{20.185}{25}\right)}{\log\left(\frac{25}{20}\right)} + 1.119$$

$$\alpha v20 = (1.054 - 1.084)\cdot - \frac{\log\left(\frac{20.185}{25}\right)}{\log\left(\frac{25}{20}\right)} + 1.054$$

$$k20 = \frac{(kh20 + kv20) + (kh20 - kv20)\cdot\cos(\theta)^2\cdot\cos(\tau\cdot 2)}{2}$$

$k20 = 0.0630989053$

$$\alpha 20 = \frac{kh20\cdot\alpha h20 + kv20\cdot\alpha v20 + (kh20\cdot\alpha h20 - kv20\cdot\alpha v20)\cdot\cos(\theta)^2\cdot\cos(2\cdot\tau)}{2\cdot k20}$$

$\alpha 20 = 1.0710708332$

$$kh27 := 10^{\left(\log\left(\frac{.1811}{.1159}\right)\cdot\frac{\log\left(\frac{27.505}{25}\right)}{\log\left(\frac{30}{25}\right)}+\log(0.\ \ 59)\right)}$$

$$kv27 := 10^{\left(\log\left(\frac{.159}{.1028}\right)\cdot\frac{\log\left(\frac{27.505}{25}\right)}{\log\left(\frac{30}{25}\right)}+\log(0.1028)\right)}$$

$$\alpha h27 := (1.0\ \ 5\ \ \ 1.081)\cdot-\frac{\log\left(\frac{27.505}{25}\right)}{\log\left(\frac{30}{25}\right)}\ \ \ .035$$

$$\alpha v27\ \ (1.018-\ \ .054)\cdot-\frac{\log\left(\frac{27.505}{25}\right)}{\log\left(\frac{30}{25}\right)}\ \ 1\ \ .018$$

$$k27\ \ \frac{(kh27-\ \ kv27)+(kh27\cdot\ \ kv27)\cdot\cos(\theta)^2\cdot\cos(\tau\cdot 2)}{2}$$

$k27\ \ 0.1311683662$

$$\alpha 27 := \frac{kh27\cdot\alpha h27+kv27\cdot\alpha v27+(kh27\cdot\alpha h27-\ \ kv27\cdot\alpha v27)\cdot\cos(\theta)^2\cdot\cos(2\cdot\tau)}{2\cdot k27}$$

$\alpha 27 := 1.0006591497$

APPENDIX B - Calculation of CCIR-Defined Gaseous Attenuation

CCIR Gaseous (Oxygen & Water Vapor) Attenuation Model Equations for f = 57 GHz

$$\alpha_o = \left[7.19\cdot10^{-3}+\frac{6.09}{f^2+0.227}+\frac{4.81}{(f-57)^2+1.15}\right]f^2\cdot10^{-3}\left[\frac{dB}{km}\right]$$

$$\alpha_w = \left[0.05+0.0021\cdot\rho+\frac{3.6}{(f-22.2)^2+8.5}+\frac{10.6}{(f-183.3)^2+9}+\frac{8.9}{(f-325.4)^2+26.3}\right]f^2\cdot\rho\cdot10^{-4}\left[\frac{dB}{km}\right]$$

$$h_o = 6\ km \qquad h_w = h_{wO}\left[1+\frac{.3}{(f-22.2)^2+5}+\frac{.5}{(f-183.3)^2+6}+\frac{2.5}{(f-325.4)^2+4}\right]\ (km)$$

where: h_{wO} = 1.6 km (clear weather) = 2.1 km (rain)

$$R_w = 461\left[\frac{joule}{kg\cdot K}\right]$$

$$\rho = RH\cdot\frac{e_s}{R_w\cdot(1+273)}\left[\frac{g}{m^3}\right] \qquad e_s = \frac{5854\cdot10^{\left(20-\frac{2050}{273+T}\right)}}{(273+T)^5}\ (millibars) \qquad RH = Relative\ Humidity\ \ \%$$

Correction Factors for Temperature Variances (Stated Range of Accuracy -20 °C to 40 °C)

$\alpha_{oZ} = \alpha_o - 0.01\cdot\alpha_o\cdot(T-15\ °C)$ $\qquad$ $\alpha_{wZ} = \alpha_w - 0.01\cdot\alpha_w\cdot(T-15\ °C)$

$h_{oZ} = h_o - 0.01\cdot h_o\cdot(T-15\ °C)$ $\qquad$ $h_{wZ} = h_w - 0.01\cdot h_w\cdot(T-15\ °C)$

Zenith Attenuation: $A_Z = \alpha_o\cdot h_o + \alpha_w\cdot h_w$

Correction for Non-Zenith Propagation Paths With Elevation Angles θ < 10°

$$A_\theta = \frac{\sqrt{R}}{\cos(\theta)}\left[\alpha_o\sqrt{h_o}\cdot F\left[\tan(\theta)\sqrt{\frac{R}{h_o}}\right]+\alpha_w\sqrt{h_w}\cdot F\left[\tan(\theta)\sqrt{\frac{R}{h_w}}\right]\right]\ (dB)$$

where: $F(x) = \frac{1}{0.661\cdot x+0.339\sqrt{x^2+5.51}}$

APPENDIX C - (‘calculation of CCIR-Defined Rain Attenuation

CCIR Rain Attenuation Model Equations For ACTS Beacons (20.185 GHz Shown):

Evaluation of Site Tilt Angle τ: $\alpha \equiv$ Earth_Station_Latitude $\beta \equiv$ Satellite_Longitude − Earth_Station_Longiude

$\tau := \operatorname{atan}\left[\frac{\tan(\alpha)}{\sin(\beta)}\right]$ $\tau = 70.70093 \cdot \text{deg}$ $\alpha \equiv 64.7 \cdot \text{deg}$ $\beta \equiv (360 - 100) \cdot \text{deg} - (360 - 147.8) \cdot \text{deg}$

(+ Northern Hemisphere) (Measured in Degrees East)

$\theta \equiv 8 \text{ deg}$ (Elevation Angle)

Calculate the Regression Coefficients Used in The Calculations, k and α.

$k_{1H} \equiv 0.0751$ $k_{2H} \equiv 0.124$ $f_1 \equiv 20$ $f_2 \equiv 25$ $\alpha_{1H} \equiv 1.099$ $\alpha_{2H} \equiv 1.061$

$k_{1V} \equiv 0.0691$ $k_{2V} \equiv 0.113$ $\alpha_{1V} \equiv 1.065$ $\alpha_{2V} \equiv 1.030$

$$k_H := 10^{\left[\log\left[\frac{k_{2H}}{k_{1H}}\right]\frac{\log\left[\frac{20.185}{f_1}\right]}{\log\left[\frac{f_2}{f_1}\right]} + \log(k_{1H})\right]}$$

$k_H = 0.07667$

$$k_V := 10^{\left[\log\left[\frac{k_{2V}}{k_{1V}}\right]\frac{\log\left[\frac{20.185}{f_1}\right]}{\log\left[\frac{f_2}{f_1}\right]} + \log(k_{1V})\right]}$$

$k_V = 0.07052$

$$\alpha_H := (\alpha_{2H} - \alpha_{1H})\frac{\log\left[\frac{20.185}{f_1}\right]}{\log\left[\frac{f_2}{f_1}\right]} + \alpha_{1H}$$

$\alpha_H = 1.09743$

$$\alpha_V := (\alpha_{2V} - \alpha_{1V})\frac{\log\left[\frac{20.185}{f_1}\right]}{\log\left[\frac{f_2}{f_1}\right]} + \alpha_{1V}$$

$\alpha_V = 1.06356$

$$k_{20185} := \frac{k_H + k_V + (k_H - k_V)\cos(\theta)^2\cos(2\tau)}{2}$$

$k_{20185} = 007119$

$$\alpha_{20185} := \frac{k_H\alpha_H + k_V\alpha_V + (k_H\alpha_H - k_V\alpha_V)\left(\cos(\theta)^2\cos(2\tau)\right)}{2 \cdot k_{20185}}$$

Values (H, α & k:

$\alpha_{20185} = 1.06754$

Site Information: $\phi \equiv 64.7$ (Station Latitude)

$\theta \equiv 8 \cdot \text{deg}$ (Elevation Angle)

$h_s \equiv 580 \cdot m$ (Station Elevation)

Calculations:

Find the freezing height during rain (h_{fr}):

$h_{fr} := [5.0 - 0.075 \cdot (\phi - 23)] \cdot \text{km}$ (For Latitudes > 23°)

Find the effective path length (L_S): $h_{fr} - h_s = 4.696 \cdot \text{km}$

$$L_S := \frac{(h_{fr} - h_s)}{\sin(\theta)}$$

$L_S = 12.184 \cdot \text{km}$

APPENDIX D - Calculation of Cloud Attenuation

Specific attenuation due to clouds is of the form: $\gamma_c(f) = 0.182 \cdot f \cdot N''_w(f) \left(\frac{dB}{km}\right)$

Where: f = frequency in GHz

N''_w is the imaginary part of the complex refractivity in ppm (10^{-6}) $N''_w = \frac{9}{2} \frac{w}{\varepsilon'' \left(1 + \eta^2\right)}$

Where w is the liquid water density in g/m^3 and $\eta = \frac{\left(2 + \varepsilon'\right)}{\varepsilon''}$

Where ε' and ε'' are the real and imaginary parts of the permittivity of water
(The double Debye relaxation model gives the dielectric spectra for water as below)

$$\varepsilon'(f) = \varepsilon_2 + \frac{\varepsilon_0 - \varepsilon_1}{1 + \left(\frac{f}{f_p}\right)^2} + \frac{\varepsilon_1 - \varepsilon_2}{1 + \left(\frac{f}{f_s}\right)^2} \qquad \varepsilon''(f) = \frac{f\left(\varepsilon_0 - \varepsilon_1\right)}{f_p\left[1 + \left(\frac{f}{f_p}\right)^2\right]} + \frac{f\left(\varepsilon_1 - \varepsilon_2\right)}{f_s\left[1 + \left(\frac{f}{f_s}\right)^2\right]}$$

Where:

f = frequency (GHz) $\varepsilon_0 = 77.66 + 103.3\left(\theta - 1\right)$ $\varepsilon_1 = 5.48$ $\varepsilon_2 = 3.51$

$f_p = 20.09 - 142\left(\theta - 1\right) + 294\left(\theta - 1\right)^2$ (GHz) $f_s = 590 - 1500\left(\theta - 1\right)$ (GHz)

Where $\theta = \frac{300}{T}$ and T is temperature in Kelvin

Liquid water content is found from: $w = w_0\left(1 + c\,t\right)\left(\frac{h_c}{h_r}\right)^a p_w(t) \left(\frac{g}{m^3}\right)$

Where:

w_0 is the liquid water content of the cloud $\left(\frac{g}{m^3}\right)$ $p_w(t) = \begin{cases} 1 & 0\ ^\circ C > t \\ 1 + \frac{t}{20} & 20\ ^\circ C > t > 0\ ^\circ C \\ & -20\ ^\circ C \end{cases}$

$c = 0.041 \left(\frac{1}{^\circ C}\right)$ t = Temperature (°C)

h_c = height from cloud base (m) a = .4

h = reference height (m) (In this evaluation h = h eliminating the middle term)

$$\text{Distance (km)} = \frac{\text{Effective Path(km)}}{\sin(8^\circ)}$$

$$\text{Attenuation (dB)} = \text{Distance (km)} \cdot \gamma_c(f) \left(\frac{dB}{km}\right)$$

REFERENCES

[1] Y. Karasawa, M. Yamada, and J. E. Allnutt, "A New Prediction Method for Tropospheric Scintillation on Earth-Space Paths," *IEEE Trans. Antennas Propagation.*, vol. 36, no. 11, pp. 1608-1614, Nov. 1988.

[2] ITU-R P-Series Recommendations Radiowave Propagation P.618-4, Propagation data and prediction methods required for the design of earth space telecommunications systems, International Telecommunications Union, Geneva, 1996.

[3] G. Peeters, F. Marzano, G. d'Auria, C. Riva, and D. Vanhoenacker-Janvier "Evaluation of Statistical Models for Clear-Air Scintillation Prediction using Olympus Satellite Measurements," *Int'l Journal of Satellite Communications*, vol. 15, pp. 73-88, 1997.

[4] J. Tervonen, M. van de Kamp, and E. Salonen, "Prediction Model for the Diurnal Behavior of the Tropospheric Scintillation Variance," *IEEE Trans. Antennas Propagation.*, vol. 46, no. 9, pp. 1372-1378, Sep. 1998.

[5] R. Singleton, "A Method for Computing the Fast Fourier Transform with Auxiliary Memory and Limited High-Speed Storage," *IEEE Transactions on Audio and Electroacoustics*, vol. AU-15, no. 2, pp. 91-98, Jun. 1967

[6] E. Matricciani, "Prediction of Fade Durations Due to Rain in Satellite Communications", *Science*, vol. 32, no. 3, pp. 935-941.

[7] E. Matricciani, "Physical-mathematical Model of the Dynamics of Rain Attenuation Based on Rain Rate Time Series and a TWO-layer Vertical Structure of Precipitation," *Radio Science*, vol. 31, no. 2., pp. 281-295, Mar.-Apr. 1996.

[8] W. H. Press, S. A. Teukolsky, W. T. Vetterling, B. P. Flannery, *Numerical Recipes in C - The Art of Scientific Computing*, 2nd ed. New York: Cambridge, 1992, pp. 532-5.36.

[9] D. Maggiori, "Computed Transmission through Rain in the 1-400 GHz Frequency Range for Spherical and Elliptical Drops and Any Polarization," *Alta Frequenza*, Vol. L, No. 5, Sep.-Oct. 1981, pp. 262-273.

[10] A. Paraboni, C. Riva, "A New Method for the Prediction of Fade Duration Statistics in Satellite Links Above 10 GHz," *International Journal of Satellite Communications*, vol. 12, pp. 387-394, 1994.

[11] R. M. Manning, "Fade Dynamics and its Evolution: The Other Part of the ACTS Rain Prediction Model," *Proceedings of the Twenty-First NASA Propagation Experimenters Meeting*, pp. 2-23 to 2-40, Aug. 1997.

[12] R. M. Manning, "A Unified Statistical Rain-Attenuation Model for Communication Link Fade Predactions and Optimal Stochastic Fade Control Design Using a Location Dependent Rain-Statistics Database," *International Journal of Satellite Communications, vol. 8, pp. 11-30, 1990.*

[13] T. Maseng, P. M. Bakken, "A Stochastic Dynamic Model of Rain Attenuation," *IEEE Trans. on Comm.*, vol. COM-29, no. 5, pp. 660-669.

[14] G. Brussard & P. A. Watson, "Atmospheric Modeling and Millimetre Wave Propagation", Chapman & Hall, First Edition 1995, pp. 2129

[15] J. E. Allnut, "Satellite-to-Ground Radiowave Propagation: Theory, Practice and System Impact at Frequencies Above 1 GHz", Peter Peregrinus Ltd, 1989.

[16] Asoka Dissanayake, "A Prediction Model that Combines Rain Attenuation and Other Propagation Impairments Along Earth-Satellite Paths", IEEE Transactions on Antennas and Propagation, Vol. 45, No. 10 October 1997.

[17] Stephen D. Slobin, "Microwave Noise temperature and Attenuation of clouds: Statistics of These Effects at Various Sites in the United States, Alaska, and Hawaii", Radio Science, Vol. 17, No. 6 November-December 1982.

[18] E. Salonen & S. Uppala, "New Prediction Method of Cloud Attenuation", Electronics Letters, Vol. 27 No. 12, 6th June 1991.

[19] Hans J. Liebe, "MPM - An Atmospheric Millimeter-Wave Propagation Model", National Journal of Infrared and Millimeter Waves, Vol. 10 No. 6 1989.